ORIGINAL PAPER

Preparation, characterization and thermal properties of polypropylene/polyethylene/zinc borate composites: investigation of thermal degradation kinetics

Fehmi Saltan[1,2] · Semih Şentürk[2] · Ayça Mehmetoğlu Al[3] · Ayşe Nur Özkan[1,4] · Kamil Şirin[2]

Abstract

In this study, polypropylene/polyethylene/zincborate composites (PP/HDPE/Zinc Borate) were prepared using high-density polyethylene, isotactic polypropylene, and a certain percentage of zinc borate. The composites were characterized using by X-Ray Diffraction (XRD), Scanning Electron Microscopy-Energy Dispersive Spectroscopy (SEM-EDX), Fourier Transform Infrared (FT-IR) spectroscopy analyses. The thermal behavior of the materials was investigated using thermogravimetric analysis (TG), Differential Thermal Analysis (DTA), and Differential Thermogravimetry (DTG). The thermal degradation kinetics of the PP/HDPE/Zinc Borate$_{15\%}$ composite was investigated. The apparent activation energies (E_a) were obtained following the differential and integral methods of Kissenger and Flynn-Wall-Ozawa (FWO). Using Kissinger's and Flynn–Wall–Ozawa methods to define thermal degradation of PP/HDPE/Zinc Borate$_{\%15}$, their activation energies were 233.3 kJ/mol and 189.3 kJ/mol, respectively. The mechanism of the studied conversion range was found to be the R3 deceleration model using the Coats–Redfern. The viscosity and shear stress of PP/HDPE/Zinc Borate$_{15\%}$ were determined using a cone-plate type rheometer. PP/HDPE/Zinc Borate$_{15\%}$ composite shows plastic-type fluidity, according to rheological analysis.

Keywords Polypropylene · Polyethylene · Zinc Borate · Thermal Degradation Kinetic · Characterization

Introduction

As general thermoplastics, polypropylene (PP) and polyethylene (PE) have been widely used in many fields because of their outstanding chemical stability, low price, processability, and high-temperature resistance [1, 2] and as known, commercial PE and PP have been used as mixtures in material production for many years because of their superior properties [3, 4]. Although preparing these mixtures is a solution to many problems, some important deficiencies cannot be eliminated. Composites have been prepared with some inorganic materials to overcome the shortcomings of PP/PE blends in the literature and for industrial applications, and to gain new and superior properties [5, 6]. Zinc borate is commonly used as a flame retardant in the cellulose fiber, rubber, plastic, textile, and paper industries. They are also used in pigments, paints, and adhesives. Frequently used commercial polymers such as polyethylene and polypropylene can easily form molten drops or catch fire in the case of possible combustion. By adding zinc borate to this type of material, carbon chains are supported and easy melting is prevented. Even when heated above a certain temperature, it preserves the integrity of the material to which it is added and maintains its flame retardant effect. Zinc borate is a halogen-free, environmentally friendly, flame retardant with high thermal stability [7–9]. Considering the usage areas and quantities, it is very important to prepare blend composites, as in this study, for the recovery and reuse of PE and PP, which have high plastic waste rates.

Although PE/zinc borate and PP/zincborate composites are primarily studied as flame retardants, data on their degradation kinetics are scarce [10, 11]. As it is known, the degradation of commercially prepared polymeric composites is the focus

✉ Fehmi Saltan
fehmisaltan@hotmail.com

1   Faculty of Science, Department of Chemistry, Cankiri Karatekin University, 18100, Merkez, Çankiri, Turkey

2   Faculty of Art and Science, Department of Chemistry, Manisa Celal Bayar University, 45140, Yunusemre, Manisa, Turkey

3   Faculty of Science, Department of Chemistry, Ege University, 35040, Bornova, İzmir, Turkey

4   Manisa Celal Bayar University, Applied Science Research Center (ASRC), 45140 Yunusemre, Manisa, Turkey

of many studies on materials management. In addition, the analysis of the degradation kinetics of polymeric materials is very important for modeling the degradation process [12, 13]. It is thought that the thermal degradation kinetics of the PP/HDPE/Zincoborate composite presented in this study will contribute to the processing of similar materials prepared in previous studies.

In this study, PP/HDPE/Zincoborate polymer composites were prepared and reported for the first time in the literature. The thermal stability of zinc borates added at different percentages to the polymer blend was investigated. Thermal degradation kinetics were investigated using integral (Flynn–Wall–Ozawa (FWO), Coats–Redfern method) and differential (Kissinger) methods for the composite with the highest thermal resistance. The apparent activation energies for the thermal degradation of PP/HDPE/ZincBorate were obtained using Kissinger, FWO, and Coats methods.

Kinetic analysis

Throughout modern history, many investigators have been interested in the kinetic analysis of thermal decomposition processes. Thermal decomposition causes kinetics to be vital for explaining any sample undergoing thermal decomposition; kinetics are also intrinsically linked to the mechanisms underlying decomposition. To postulate the mechanisms for thermal decomposition, we must have a thorough understanding of the mechanism or vice versa. In addition, kinetic equations can be used to postulate the mechanisms of thermal decomposition. To obtain the kinetic parameters, such as the reaction rate, activation energy and pre-exponential factor, it is necessary to first determine the appropriate equation based on kinetics mechanism studies [14, 15].

As follows:

$$d\alpha/dt = (1/\beta)Ae^{-(E_a/RT)}f(\alpha) \tag{1}$$

Several methods for the calculation of kinetic parameters A, E_a, and α based on integral or differential methods are used, where β is the heating rate (β = dT/dt), A is the pre-exponential factor, E_a is the activation energy, R is the gas constant, and the fractional conversion α is expressed as a function of temperature.

Differential method

Kissinger method In simplest terms equation for approximation, the activation energy, E_a, is as follows [16–18]:

$$E = -R\frac{dIn\left(\frac{\beta}{T_{max}^2}\right)}{dT_{max}^{-1}} \tag{2}$$

where R is the gas constant, β is the heating rate, and T_{max} is the temperature corresponding to the position of the rate peak maximum. Most commonly, T_{max} is determined as the temperature of the peak signal (maximum or minimum) measured by DSC, DTA or (DTG).

A more informative form of the Kissinger equation is the integral:

$$In\left(\frac{\beta}{T_{max}^2}\right) = In\left(\frac{AR}{E_a}\right) + In\left(n(1-\alpha_{max})^{n-1} - (\frac{E}{RT_{max}})\right) \tag{3}$$

where A is the pre-exponential factor, α_{max} is the maximum degradation fraction, and n is the reaction order.

According to the Kissenger method, the plots of $In(\beta/T_{max}^2)$ versus $(1000/T_{max})$ can yield straight lines with a slope equal to $-E_a/R$.

Integral methods

Flynn-Wall-Ozawa method can be used to calculate the activation energy of a decomposition process without knowing the reaction order and differential data of the TGA [19, 20]. In Eq. (4), the integration from T_o, which corresponds to the degree of conversion α_0, to T_{max}, where $\alpha = \alpha_{max}$, yields:

$$g(\alpha) = \int_{\alpha_o}^{a_{max}} \frac{d\alpha}{f(\alpha)} = \frac{A}{\beta}\int_{T_0}^{T_{max}} \exp\left(\frac{E}{RT}\right)dT \tag{4}$$

where $g(\alpha)$ represents the integral function of the conversion. Assuming that $\alpha = E_a/RT$, Eq. (4) can be written as:

$$\frac{A}{\beta}\int_{T_0}^{T_{max}} \exp\left(\frac{E}{RT}\right)dT = \frac{AE}{\beta R}p(x) \tag{5}$$

Ozawa's method is based on Doyle's approximation.
Log $p(x) \approx 2.315 - 0.457x$
Or ln$p(x) \approx 5.330 - 1.052x$
The equation can be written as:

$$\log \beta = \log \frac{AE_a}{g(\alpha)R} - 2.315 - \frac{0.4567E}{RT} \tag{6}$$

In this case, A and R are constants, and g(α) is also constant for any given conversion. Therefore, the value of E can be calculated using Ozawa's method for any given degree of dissociation by determining the linear dependence of the log β versus $1/T$ plot at different heating rates, without knowing the reaction order.

Coats-Redfern method The order of reactions is frequently preticted using a model-fitting method, the Coats-Redfern model. The basic equation for coats- Redfern method is given below [21, 22];

$$In (g(\alpha)/T^2) = In (AR/(E_a\beta)) - (E_a/RT) \tag{7}$$

Table 1 Algebraic Expressions of g(α) for the Most Frequently Used Mechanisms of Solid-State Processe [22–24]

Symbol	Solid-State Processes	$g(\alpha)$
A_2	Nucleation and growth	$[-\ln(1-\alpha)]^{1/2}$
A_3	Nucleation and growth	$[-\ln(1-\alpha)]^{1/3}$
A_4	Nucleation and growth	$[-\ln(1-\alpha)]^{1/4}$
R_1	Phase boundary controlled reaction (one-dimensional movement)	α
R_2	Phase boundary controlled reaction (Contracting area)	$[1-(1-\alpha)^{1/2}]$
R_3	Phase boundary controlled reaction (Contracting volume)	$[1-(1-\alpha)^{1/3}]$
D1	One-dimensional diffusion	α^2
D2	Two-dimensional diffusion (bidimensional particle shape) Valensi equation	$(1-\alpha).\ln(1-\alpha)+\alpha$
D3	Three-dimensional diffusion (tridimensional particle shape) Jander equation	$[1-(1-\alpha)^{1/3}]^2$
D4	Three-dimensional diffusion (tridimensional particle shape) Ginstling–Brounshtein	$(1-2\alpha/3)-(1-\alpha)^{2/3}$
F_1	Random nucleation with two nucleus on the individual particle	$-\ln(1-\alpha)$
F_2	Random nucleation with two nucleus on the individual particle	$(1-\alpha)^{-1}-1$
F_3	Random nucleation with two nucleus on the individual particle	$(1/2)[(1-\alpha)^{-2}-1$

where β represents the heating rate, R represents the universal constant (0.008314 kJ/mol) and g(α) is a kinetic function of the different reaction mechanisms obtained from the integration of f(α). The activation energy can be calculated by drawing a graph between $1000/T$ and $\ln[g(\alpha)/T^2]$ and calculating the slope from the straight line drawn. The solid-state reactions can be described using the reaction models presented in Table 1 [23–25].

Experimental

Materials

Polypropylene (isotactic, Mn=67,000, Sigma-Aldrich), Polyethylene (High density, melt index 12 g/10 min (190 °C/2.16kg), Zinc Borate ($2ZnO \cdot 3B_2O_3 \cdot 3.5H_2O$, 95%, TEKKİM), p-Xylene (anhydrous, ≥99%, Sigma-Aldrich)

Instrumentations

Fourier transform infrared spectroscopy (FTIR) spectra were recorded on a PerkinElmer FTIR Spectrum One-B spectrometer (USA), XRD (X-Ray Diffraction) XRD (X-Ray Diffraction) analysis was performed with a Thermo Scientific ARL K-Alpha, X-ray source: Cu-Kα, Normal scan speed: (0.1° 2θ/s), Cu radiation 1.5406 A° (0,15406 nm). All scanning electron microscopy (SEM)images were obtained using a field emission scanning electron microscope Thermo Scientific Apreo S SEM under a high vacuum at a voltage of 15.0 kV and a working distance of 6.0 mm.

The related samples were coated with AuPd alloy for SEM and EDX analysis by sputter coating in a 100 s diffuse technique. Images of the coated samples were obtained using an in-column secondary electron detector in the reference Polaroid 545 at an acceleration voltage of 15 kV under a high vacuum. EDX analyses were performed using a 129 keV electron detector in the visible region. Images and EDX analyses were obtained with a 30 μm aperture aperture, scanning speed of 5.4 seconds for a 1024x768 pixel image. Thermogravimetry (TG) measurements of the polymer nanocomposites were obtained on a PerkinElmer Diamond TA/TGA (USA) from 25 °C to 600 °C at 10 °C a heating rate at a constant flow rate of 100 mLmin^{-1} under nitrogen atmosphere.

A cone-plate rheometer was used to observe the shear viscosity and shear stress of the compatibilized PP/HDPE/ZincBorate$_{15\%}$ composite. Lamy Rheology Instrumenets
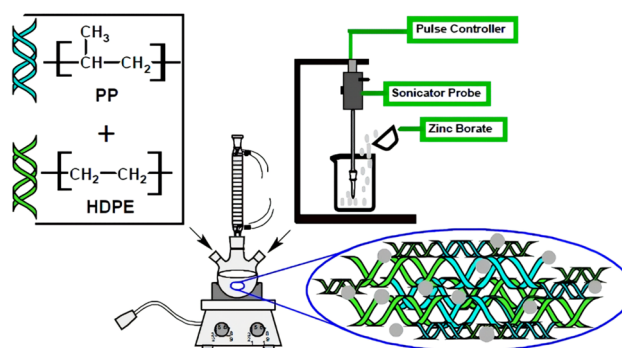

Fig. 1 Preparation of PP/Zinc Borate, HDPE/Zinc Borate and PP/HDPE/Zinc Borate composites

Table 2 Blending conditions in the preparation of composites

Composites	Amount (gram)			Solvent	°C	Hour
	PP	HDPE	ZincBorate			
PP/ZincBorate$_{5\%}$	1.9	-	0.1	p-Xylene	reflux	24
PP/ZincBorate$_{10\%}$	1.8	-	0.2			
PP/ZincBorate$_{15\%}$	1.7	-	0.3			
HDPE/ZincBorate$_{5\%}$	-	1.9	0.1			
HDPE/ZincBorate$_{10\%}$	-	1.8	0.2			
HDPE/ZincBorate$_{15\%}$	-	1.7	0.3			
PP/HDPE/ZincBorate$_{5\%}$	0.95	0.95	0.1			
PP/HDPE/ZincBorate$_{10\%}$	0.9	0.9	0.2			
PP/HDPE/ZincBorate$_{15\%}$	0.85	0.85	0.3			

(RM 200 CP4000 PLUS Model, FR) with CP4005 cone (40 mm, 0.5°, 12N, 2 to 0,5M mPa.s Viscosity range) was used for this purpose. The shear rates were varied from (20 to 200 s^{-1}) and (200 s^{-1} to 20) at 105 °C. Regression models were performed according to Newton's method. Rheological analysis was performed with a 50% (w/w) p-xylene suspension of the PP/HDPE/ZincBorate$_{15\%}$ derivative.

A General procedure for the preparation of composites containing zincborat

Polypropylene/zincborate (PP/ZincBorate), High Density Polyethylene/zincborate (HDPE/ZincBorate) and polypropylene/high density polyethylene/ZincBorate (PP/HDPE/ZincBorate) were prepared to contain 5%, 10% and 15%
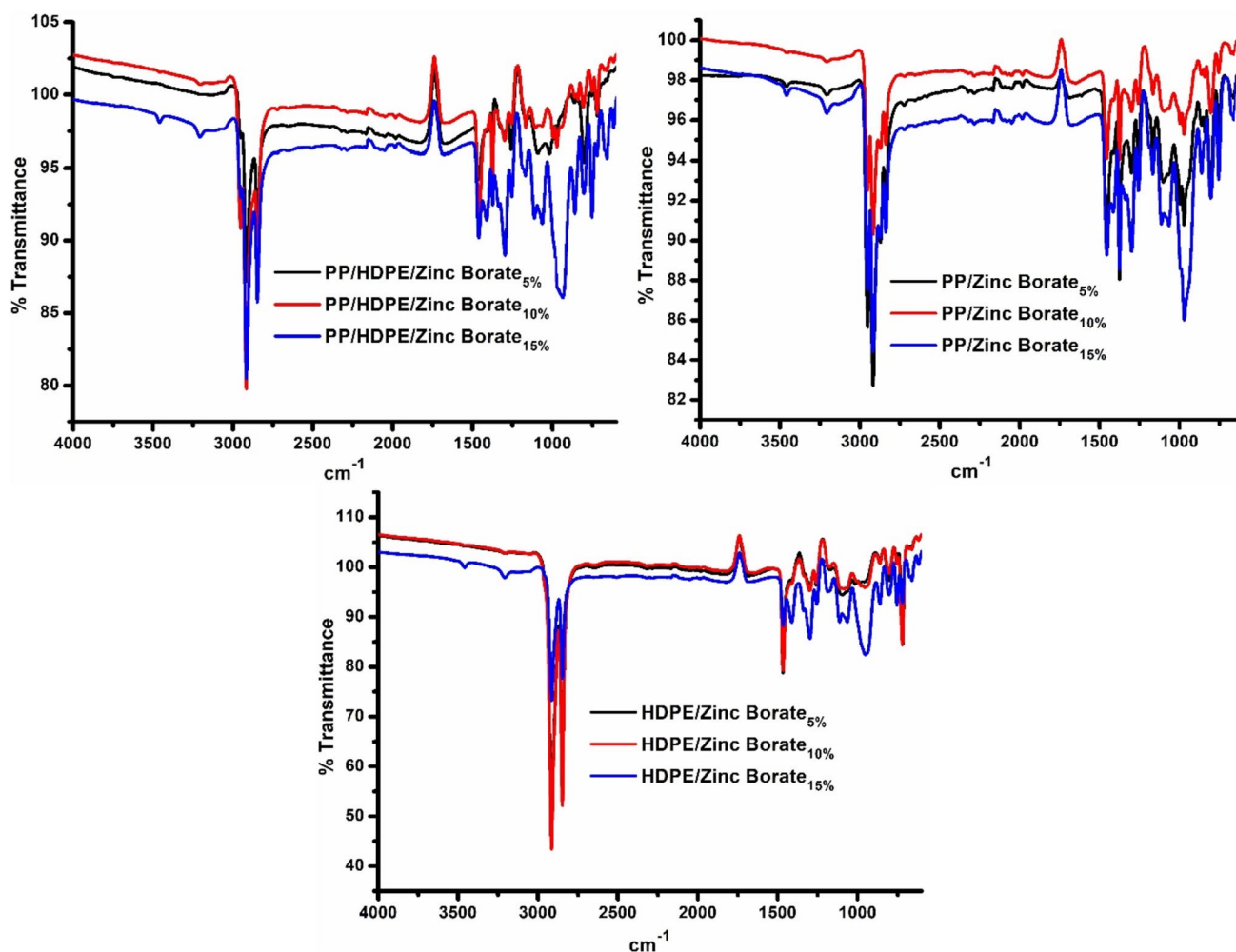

Fig. 2 FT-IR spectra of PP/Zinc Borate, HDPE/Zinc Borate and PP/HDPE/Zinc Borate composites
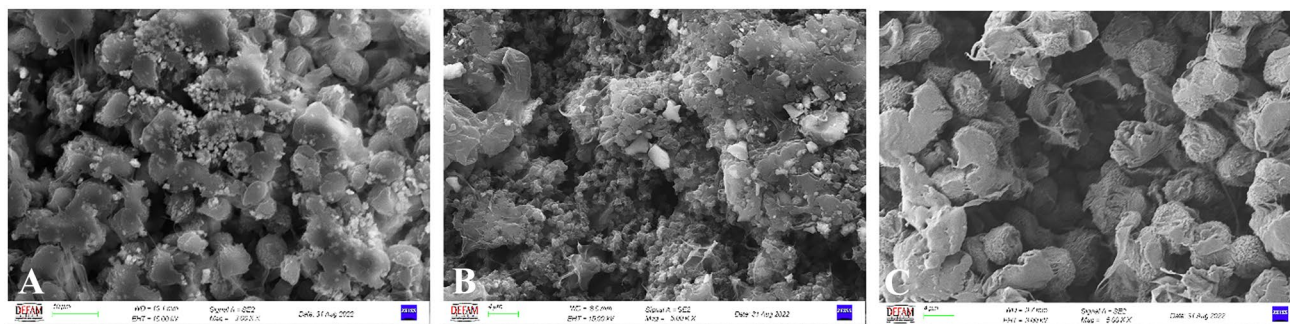
Fig. 3 SEM images of PP/HDPE/Zinc Borate composites (**A**:5%, **B**:10%, **C**:15%)

zincborates. Firstly, polymers are mixed for 2 hours at boiling temperature in p-Xylene. Zinc Borat in ethanol is kept in an ultrasonic bath for 2 h and then mixed for 2 h. A blurry white Zinc Borat suspension is added to the polymer solution and the mixture is continued at 800 rpm for 24 hours. After the solvent evaporated, the remaining solid is washed with ethanol and dried in a vacuum oven at 50 °C. The details of the composite preparation are presented in Table 2. Figure 1 schematically shows the experimental method.

Results and discussion

Surface characterization of PP/ZincBorate, HDPE/ZincBorate, and PP/HDPE/ZincBorate composites was performed by SEM analysis. The distributions of boron, carbon, zinc, and oxygen elements in the composite were examined using EDX. The crystal structures of the PP/HDPE/ZincBorate composites were elucidated by determining the 2θ diffraction angles using XRD. Their thermal behaviors were determined using TG, DTG, and DTA analyses. The thermal degradation kinetics of the PP/HDPE/Zinc Borate$_{15\%}$ composite was determined using differential and integral methods. Apparent activation energies (Ea) were calculated and interpreted. Rheological analyzes of PP/HDPE/Zinc Borate$_{15\%}$ were also performed.

FT-IR analyses

FT-IR spectra of PP/Zinc Borate, HDPE/Zinc Borate and PP/HDPE/Zinc Borate composites are shown in Fig. 2. According to Fig. 2, characteristic CH stretching of PP at 2960; 2938: 2856 cm^{-1}, CH$_2$ deformation peaks at 1460 cm^{-1} and symmetrical deformation CH$_3$ peaks at 1380 cm^{-1} can be seen clearly. The isotactic PP band can be seen at approximately 1000 cm^{-1} and 880 cm^{-1}. The C-C bending vibration of the main skeleton of PP is approximately 1180 cm^{-1} [26]. Main absorptions of HDPE in the IR region are observed in Fig. 2. These main vibrations can be described as follows (cm^{-1}): strong CH$_2$ asymmetric stretching 2930, strong CH$_2$ symmetric stretching 2815, strong bending deformations 1453 and 1433, medium wagging deformations 1386 and 1371, and medium rocking deformations 730–750 [27]. In the FT-IR spectra of PP/Zinc Borate, HDPE/Zinc Borate and PP/HDPE/Zinc Borate composites, the peaks outside the characteristic aliphatic vibration regions of PP and HDPE belong to zinc borate. The FT-IR spectrum of zinc borate used in this study is shown in Supporting Fig. 1 (SF1). In Fig. 2, the vibration of the crystal water of zinc borate and vibration of O-H groups can be seen between about 3250-3500 cm^{-1}. Due to the low percentages of zinc borate in composites and heterogeneous distribution, these peaks are of weak intensity. As expected, it is most severe in composites with 15% zinc borate. These peaks are quite weak

Table 3 Atomic percentage distribution of PP/Zinc Borate composites obtained from EDX analysis

Element	Atomic %		
	PP/ZincBorate$_{5\%}$	PP/ZincBorate$_{10\%}$	PP/ZincBorate$_{15\%}$
B	5.97	5.27	5.12
C	86.95	82.48	79.11
O	5.68	9.75	11.74
Zn	1.40	2.50	4.03

Table 4 Atomic percentage distribution of HDPE/ZincBorate composites obtained from EDX analysis

Element	Atomic %		
	HDPE/ZincBorate$_{5\%}$	HDPE/ZincBorate$_{10\%}$	HDPE/ZincBorate$_{15\%}$
B	6.54	5.66	4.97
C	86.38	81.97	82.62
O	4.96	9.05	7.91
Zn	2.12	3.32	4.50

Table 5 Atomic percentage distribution of PP/HDPE/ZincBorate composites obtained from EDX analysis

Element	Atomic %		
	PP/HDPE/ ZincBorate$_{5\%}$	PP/HDPE/ ZincBorate$_{10\%}$	PP/HDPE/ ZincBorate$_{15\%}$
B	5.57	5.15	6.78
C	84.35	81.3	71.86
O	8.68	10.12	15.84
Zn	1.40	3.43	5.52

for the composite derivatives containing 5% zinc borate. In addition, the stretching vibrations of the H-O-H bands between 1600 and 2000 cm^{-1} are due to the crystal water from zincborate. Different vibration frequencies of borate bands can also be seen in all composite derivatives in Fig. 2. Some of them can be said to be (cm^{-1}), in-plane bending of B-OH between 1250 cm^{-1}-1500 cm^{-1}, stretching vibration of the (B-O-H) from 1000 cm^{-1} to 1100 cm^{-1}, boron to oxygen bands between 800 cm^{-1}-1000 cm^{-1} [28].

SEM-EDX analyses

SEM images of PP/HDPE/Zinc Borate composites are shown in Fig. 3. SEM images of PP/Zinc Borate and HDPE/Zinc Borate composites are given in SF2 and

SF3, respectively. As it is known, smooth and flat surfaces are observed in the SEM images of pure HDPE. However, pits are seen on the surfaces in mixtures with Zinc Borate. The change in morphology, brittleness and roughness of HDPE increased as the percentage of Zinc Borate increased [29]. As in pure HDPE, SEM images of pure PP are generally observed straight without lines. On the other hand, in the SEM images of PP/Zinc Borate composites, an uneven distribution of zinc borate particles is seen on the PP surface, showing heterogeneous mixture [30]. In general, when looking at the SEM images of PP/ Zinc Borate and HDPE/Zinc Borate composites, there are agglomerates of particles distributed heterogeneously on the surface rather than the usual PP and HDPE appearances. SEM images of PP/HDPE/Zinc Borate composites show agglomerates like droplet structure, small holes as well as zinc borate fragments dispersed in the PP/HDPE matrix [31, 32].

The atomic percentages of PP/Zinc Borate, HDPE/Zinc Borate and PP/HDPE/Zinc Borate composites obtained from EDX analysis are given in Tables 3, 4 and 5, respectively. According to this table, although the atomic % results are proportional to the composition percentages of the components in the composites, there is no linear increase due to the heterogeneous distribution. As expected for all composites, although there is no linear increase as the percentage of zinc borate in the mixtures increases, the atomic percentages of zinc, boron and oxygen increase.

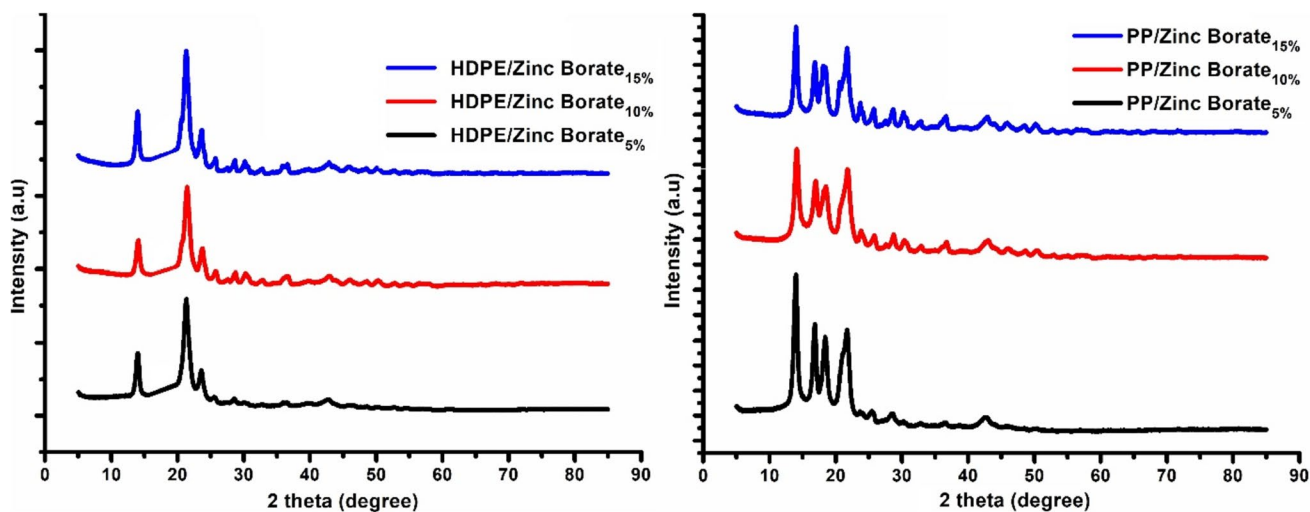**Fig. 4** XRD patterns of PP/ HDPE/Zinc Borate composites
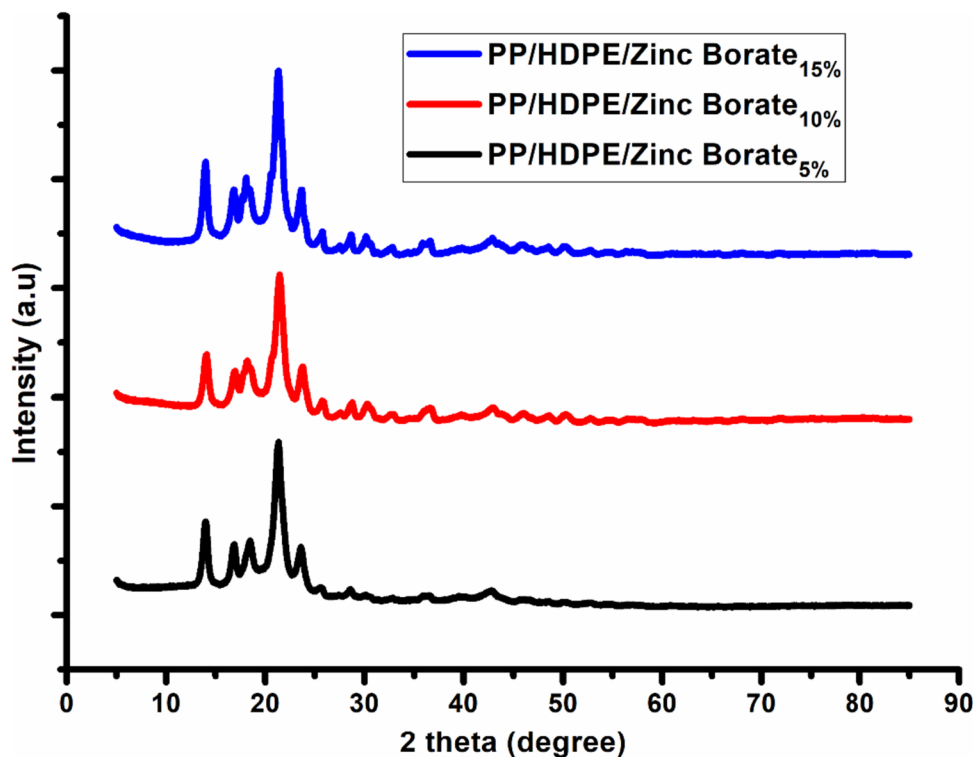
Fig. 5 XRD patterns of PP/Zinc Borate and HDPE/Zinc Borate composites

Depending on this result, the carbon atomic percentage decreases. EDX analyzes of PP/Zinc Borate, HDPE/Zinc Borate and PP/HDPE/Zinc Borate composites are shown in the Figure in SF4.

XRD analyses

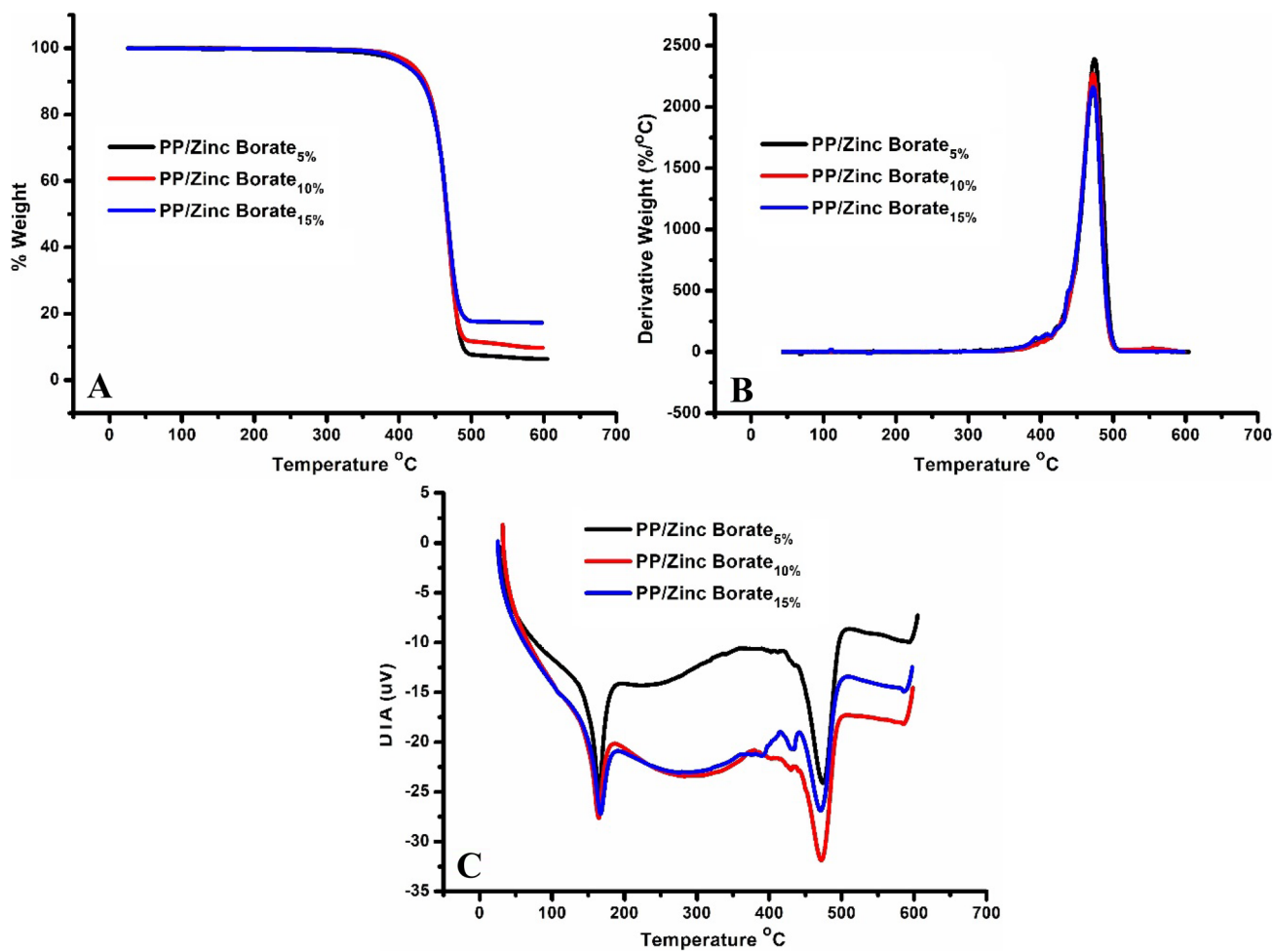Figures 4 and 5 show the XRD patterns of PP/HDPE/Zinc Borate composites and PP/Zinc Borate; HDPE/Zinc

Fig. 6 TG (**A**), DTG (**B**) and DTA (**C**) curves of PP/Zinc Borate

Borate composites, respectively. It can be seen the characteristic 2θ (2theta) diffraction angles of polyethylene, polypropylene and zincborate in these figures. According to Fig. 4, moderate and low intensity characteristic peaks of polyethylene are evident at 22° and 24º [33, 34]. The good known peaks of polypropylene at about 14°, 17º and 18° [35, 36] are clearly visible in the Fig. 4. It is possible to see diffraction peaks of different intensities between 15°-50° with it varies depending on the operating temperature and pH of Zinc Borate. The peak area where it is most intense is around 15°-25°, where the diffraction peaks of PE and PP are seen, so it is not possible to distinguish the characteristic peaks of zinc borate in this region. The other diffraction peaks of zinc borate are clearly visible at approximately 26°, 30°, 32°, 36°, 45°, 47° and 50° degrees [37, 38]. It can also be seen that the intensity of the peaks increases with the percentages of zincborate in the composite. Information about the diffraction peaks is also given on the Fig. 4. By looking at the Figs. 4 and 5, it is understood that the PP/PE/Zinc

Borate mixture shows the characteristic PE, PP and Zinc Borate diffraction peaks. The XRD results support the successful preparation of the mixture.

Thermal analyses

TG, DTA and DTG curves of PP/Zinc Borate, HDPE/Zinc Borate and PP/HDPE/Zinc Borate composites are given in Figs. 6, 7 and 8, respectively. According to Figs. 6-A, 7-A and 8-A, It was not observed important changes the thermal stabilty of the PP/Zinc Borate, HDPE/Zinc Borate and PP/HDPE/Zinc Borate composites. As expected, the thermal resistance of the composites increased proportionally with the percentage of zinc borate. In the PP/Zinc Borate, HDPE/Zinc Borate and PP/HDPE/Zinc Borate composites, the residual masses in all derivatives containing 5%, 10% and 15% zinc borate were observed to be approximately 5%, 10% and 15%. In Fig. 8-A, the remaining amounts in PP/HDPE/Zinc Borate composites containing 10% and
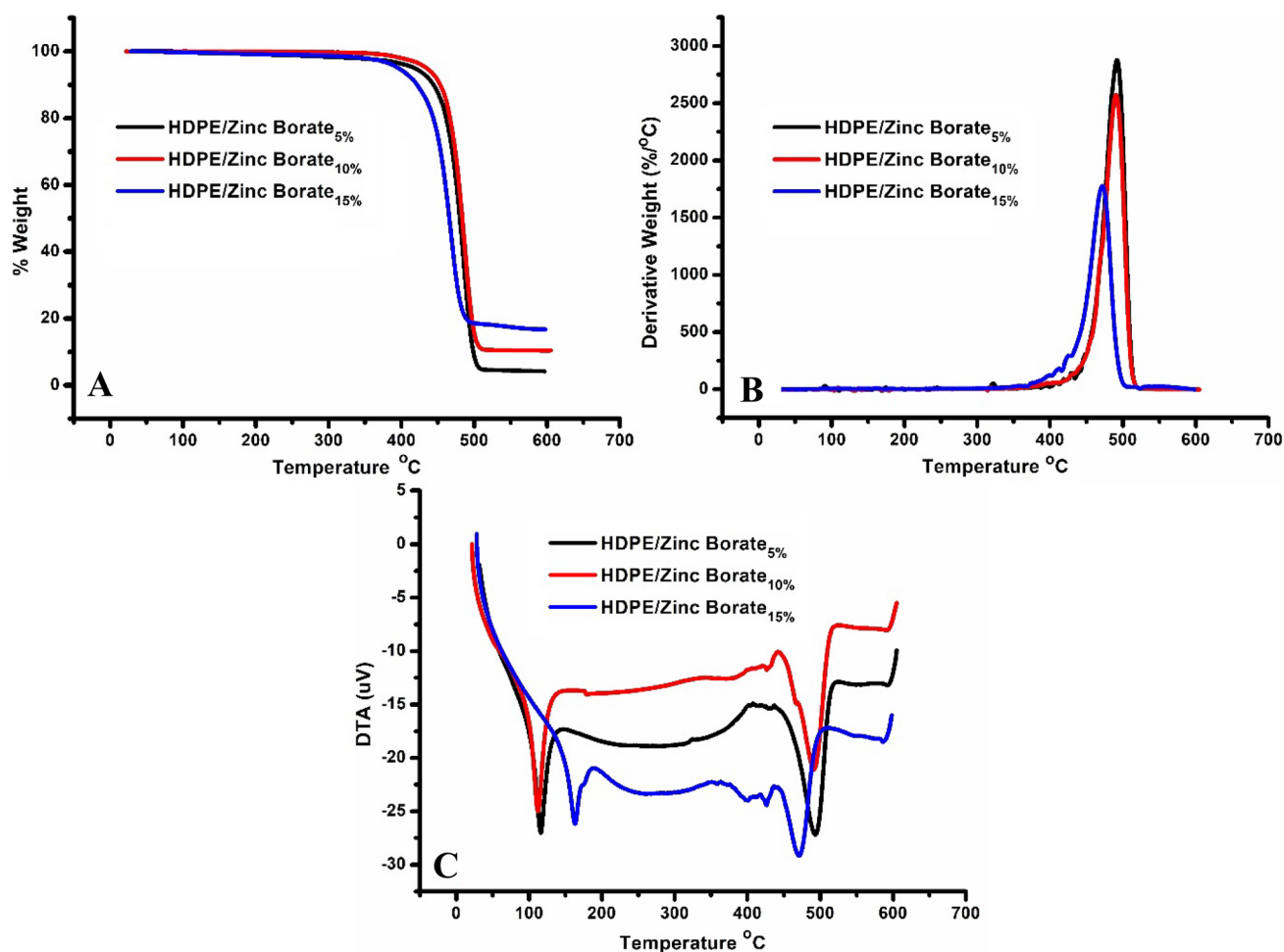

Fig. 7 TG (**A**), DTG (**B**) and DTA (**C**) curves of HDPE/Zinc Borate composites

15% zinc borate are very close unlike the other composites TG curves. The reason for this is related to the method of preparing the mixture. Although homogeneous composites with good dispersion were obtained throughout the study, homogenization was not achieved very well in PP/HDPE/Zinc Borate$_{10\%}$ and PP/HDPE/Zinc Borate$_{15\%}$ composites. Although the blending method used in the study is a cheap, accessible and easy method, it cannot provide a high rate of mixing and good dispersion as well as extrusion. As seen in Fig. 11, the polypropylene and polyethylene used in the study have no residual mass at approximately 500 °C [39]. PP, HDPE and Zinc Borate used to prepare the composites have one thermal degradation step, and similarly all composites show one degradation step. According to Fig. 11, the thermal stability of the zinc borate used in the study is lower than that of PP and PE. Therefore, the thermal stability of PP/HDPE/Zinc Borate composites is seen between zinc borate and PP/HDPE.

It is seen that in Fig. 6-B, the decomposition of PP/Zinc Borate composites starts at approximately 400 °C and the maximum decomposition temperature (T$_{max}$) is 460 °C. According to Fig. 7-B, the HDPE/Zinc Borate composites begin to decompose at about 425 °C, and the Tmax is about 490 °C. However, here, the thermal stability and T$_{max}$ value of the HDPE/Zinc Borate$_{15\%}$ derivative is lower than the other derivatives. The reason for this is the heterogeneous distribution due to the random mixture of the composites prepared in the study. When we look at the DTG curves of PP/HDPE/Zinc Borate composites in Fig. 8-B, it is seen that the decomposition starts at about 425 °C and the maximum decomposition temperature is 475 °C. The results obtained from the TG and DTG curves show that PP/HDPE/Zinc Borate composites have better thermal stability compared to PP/Zinc Borate and HDPE/Zinc Borate composites. Another conclusion to be drawn from this is that PP, HDPE and Zinc Borate, which have limited miscibility, mix successfully and
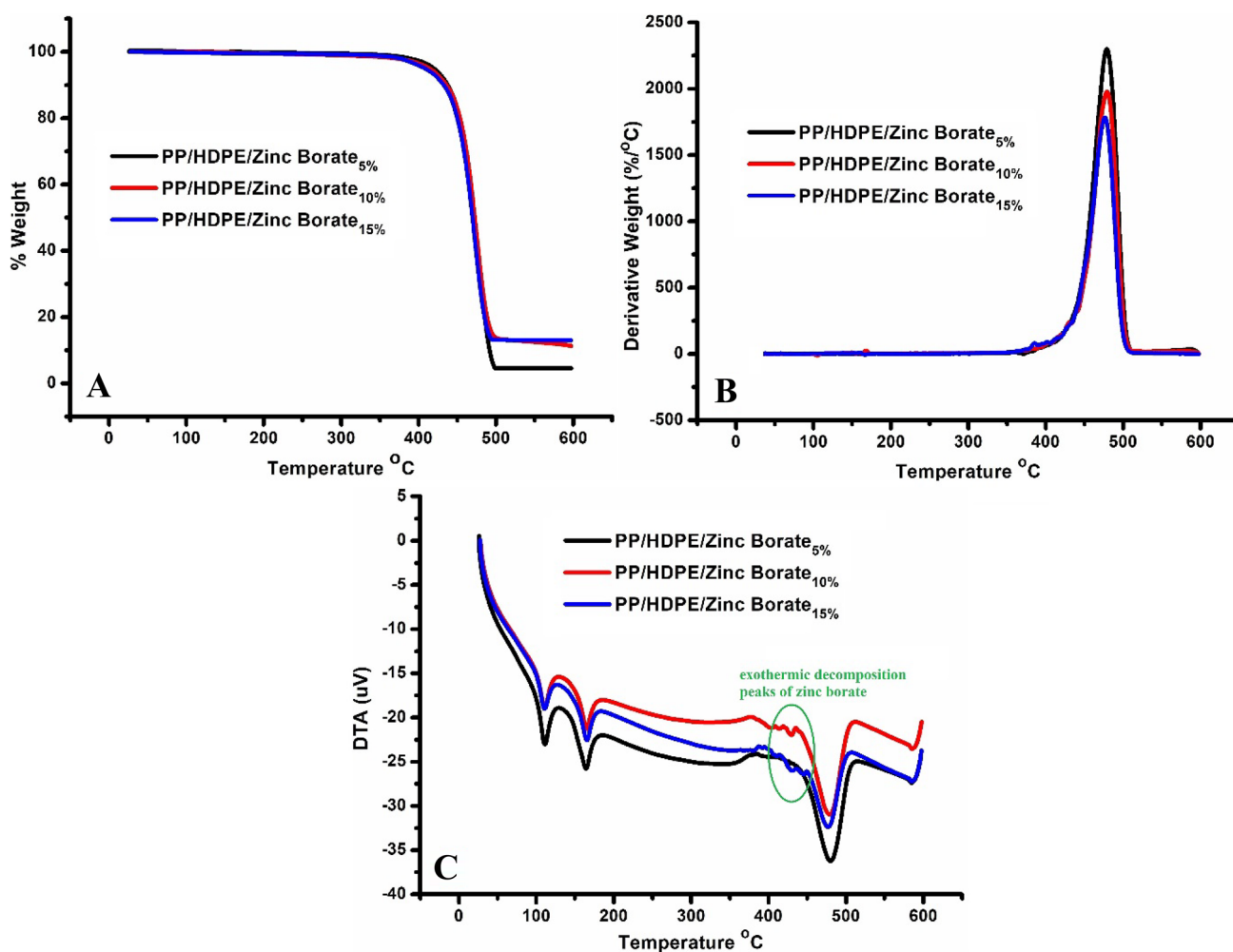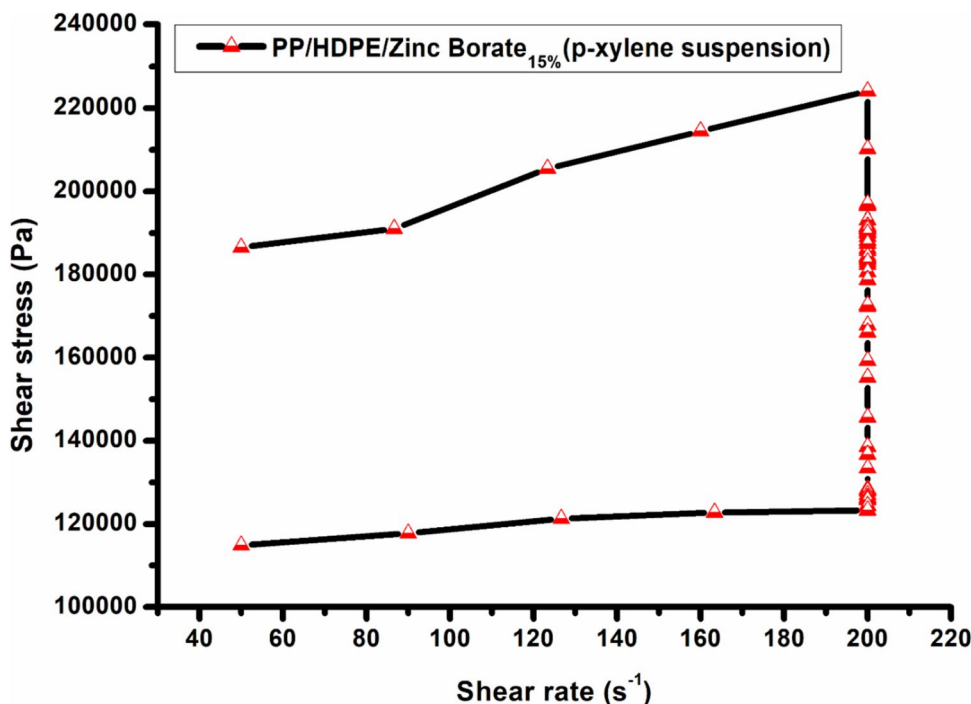

Fig. 8 TG (**A**), DTG (**B**) and DTA (**C**) curves of of PP/HDPE/Zinc Borate composites

Fig. 9 Cyclic shear rate/shear stress rheological measurement results

form a composition close to homogeneous, as supported by other characterization results.

According to Fig. 8-C, in DTA analysis of PP/HDPE/Zinc Borate composites, the existence of endothermic peaks at nearly 120 °C and 160 °C which corresponds to the crystalline phase transition of PE and PP due to melt can be observed. In addition, the mass loss corresponding to the loss of water adsorbed on the zinc borate is seen at approximately 120 °C as in HDPE. The second peak at about 480 °C corresponds to the main thermal degradation of HDPE and PP [40, 41]. Low-intensity and sequential exothermic decomposition peaks of zinc borate are observed between 420-430 °C. These low-intensity degradation peaks are more sharp in PP/HDPE/Zinc Borate10% and PP/HDPE/Zinc Borate15% derivatives than PP/HDPE/Zinc Borate5% derivative because of Zincborate percentage in composites

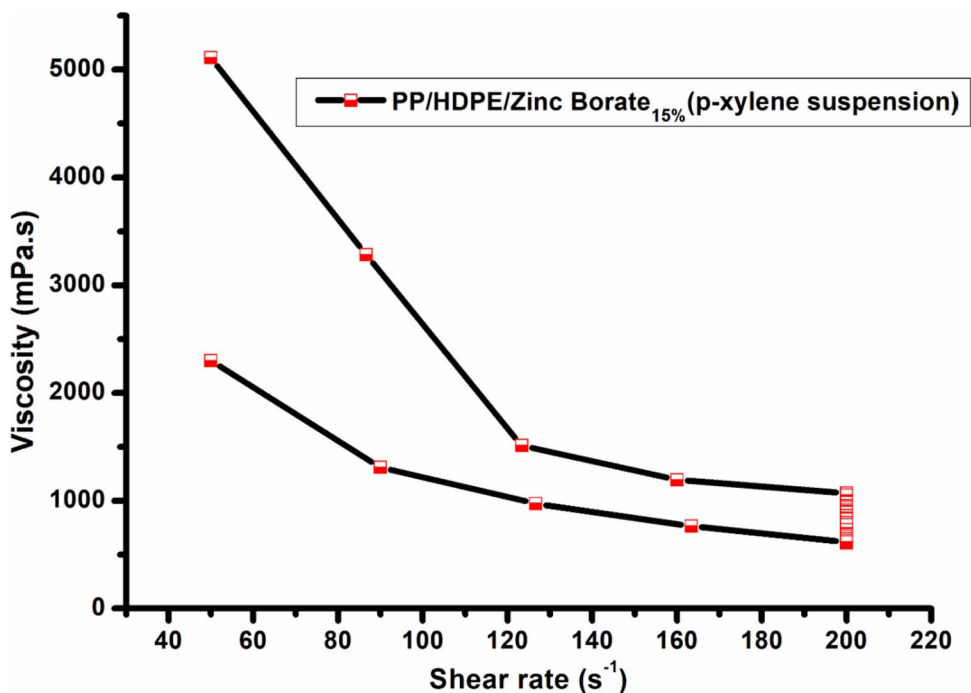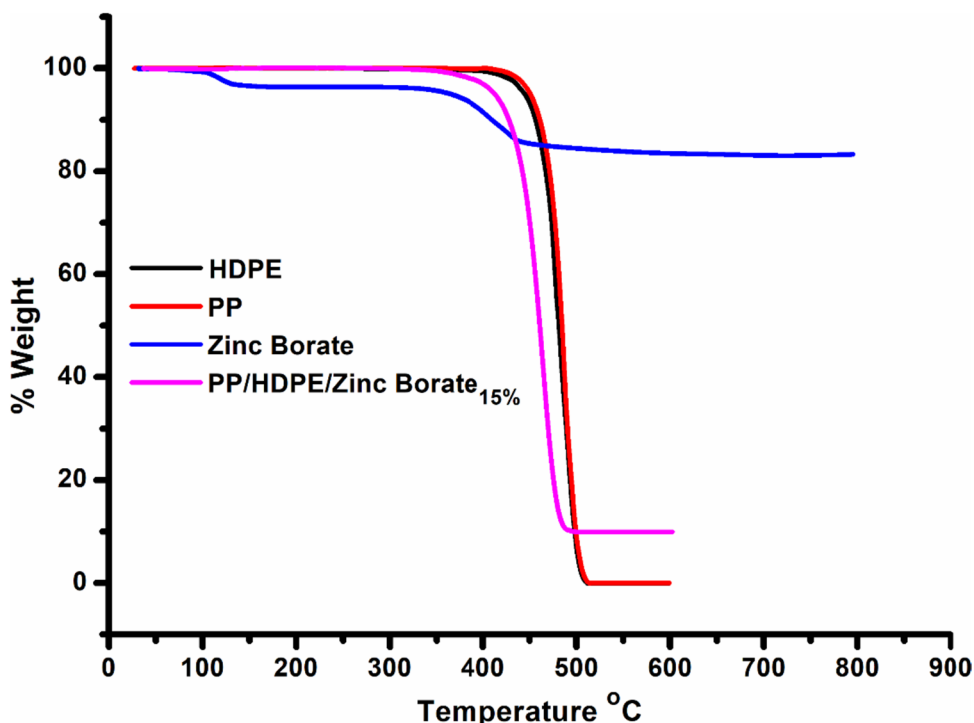**Fig. 10** Cyclic shear rate/viscosity rheological measurement results

Fig. 11 Typical TG curve PP, HDPE, Zinc Borate and PP/HDPE/Zinc Borate$_{15\%}$ in N$_2$ atmosphere at heatig rates 10 °C

as expected [42]. DTA curves of virgin PP, HDPE and Zinc Borate used in the study can be seen in SF5.

Reologic analyses of PP/HDPE/Zinc borate$_{15\%}$ composite

Figures 9 and 10 show the rheological measurements of the PP/HDPE/Zinc Borate$_{15\%}$ derivative composite. The analysis was performed at variable shear rates in cyclically and continuously conditions to determine the dynamic behavior of the composite. In the analysis, which was started to increase from 50 s^{-1} to 200 s^{-1}, the composite was analyzed at a shear

rate of 200 s^{-1} for a certain period of time. Likewise, the analysis was terminated so that the shear rate decreased from 200 s^{-1} to 50 s^{-1}. Figure 9 shows shear rate/shear stress graph and according to this figure, with the increase in shear rate, it can be clearly observed that the shear stress of the PP/HDPE/Zinc Borate$_{15\%}$ Composite increased following a non-Newtonian behavior. Non-Newtonian fluids can have a nonzero or zero yield stress. If a fluid has a non-zero yield stress, a non-zero and finite shear stress should be applied in order for the fluid to start flowing. As in this study, the simplest model describing such a fluid is the Bingham Plastic
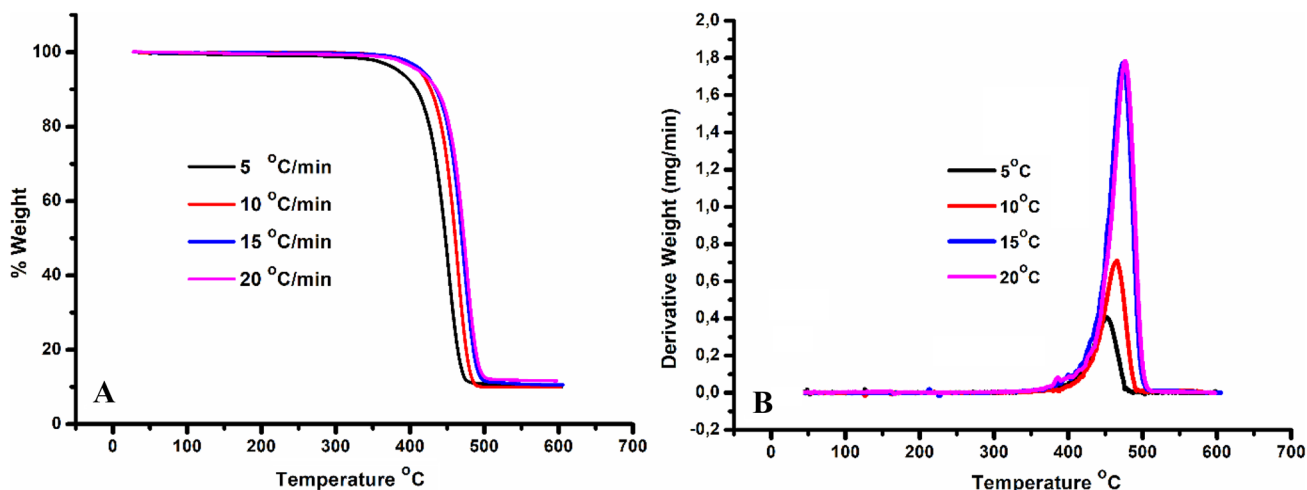

Fig. 12 (**A**) Typical TG and (**B**) DTG curves PP/HDPE/Zinc Borate$_{15\%}$ composite in N$_2$ atmosphere at heatig rates 5 °C, 10 °C, 15 °C and 20 °C

Table 6 Initial Temperature of a Decomposition Process (T_i). Maximum Degradation Temperature (T_{max}). Final Temperature of a Decomposition Process (T_f). and Residual Mass (α)

Heating Rate (β) (^oC/min)	T_i (^oC)	T_{max} (^oC)	T_f (^oC)	Residue (1 -α) at 600 °C
5	356	726.1	483	10.6
10	383	738.5	490	10.7
15	395	747.0	500	11.3
20	400	750.0	503	11.6

Model [43], where shear stress is a linear function of shear rate. Conspicuously, share stress decreases linearly at a constant shear rate of 200 s^{-1}. This can be explained by the fatigue between molecular chains. It can be observed that PP/HDPE/Zinc Borate$_{15\%}$ again showed Bingham Plastic behavior while decreasing from 200 s^{-1} shear rate to 50 s^{-1}.

Complex materials such as polymer suspensions, emulsions and solutions tend to exhibit non-Newtonian behavior. With increasing shear rate, viscosity decreases (shear thinning) or, less commonly, increases (shear thickening). These results are due to the complex microstructure and rearrangement of the material under applied pressure and are beneficial in many application areas. As seen in Fig. 10, the dynamic viscosity values of PP/HDPE/Zinc Borate$_{15\%}$ composite conform to the shear thinning profile against increasing shear rate. As expected in the cyclic analysis, the viscosity value increases with decreasing shear rate. Although lower values are read below the viscosity values

according to beginning of the analysis, these results show that the structural decomposition of the composite under a certain force is not very high. According to the curves obtained from Figs. 9 and 10, PP/HDPE/Zinc Borate$_{15\%}$ composite generally shows a plastic low probability pseudoplastic type fluidity [44]. The data of rheological analysis are given in Supporting Table 1.

Thermal degradation kinetic of PP/HDPE/Zinc borate$_{15\%}$ composite

Figures 11 and 12 is demostrated PP, HDPE, zinc borate and PP/HDPE/Zinc Borate$_{15\%}$ termograms. These termograms were taken from 30 °C to 600 °C with a heating rate of 10 °C/min at nitrogen atmosphere. The PP and HDPE have almost the same thermal stability. The mass loss of PP and HDPE begins at 442 °C and 437 °C, respectively. At 514 °C, PP and HDPE were completely decomposed and consumed. The TG curves of both PP and HDPE also indicate one reaction stage which is reflected as one degradation reaction peak. Wu et al. noted that the pure PP thermogram showed one-step decomposition in the range of 382-475 °C, and a negligible char remained above 475 °C [7]. Awad et al., on the other hand, performed thermal gravimetric analysis to examine the thermal properties of pure HDPE and HDPE composites. The HDPE thermograms obtained are in conformity with the HDPE TGs in our study [45]. It can be seen from the TG thermogram of the zinc borate molecule in Fig. 11 that there is degradation in 2 steps. The weight loss in the 100-130 °C step in

Fig. 13 Kissinger plot for PP/HDPE/Zinc Borate$_{15\%}$

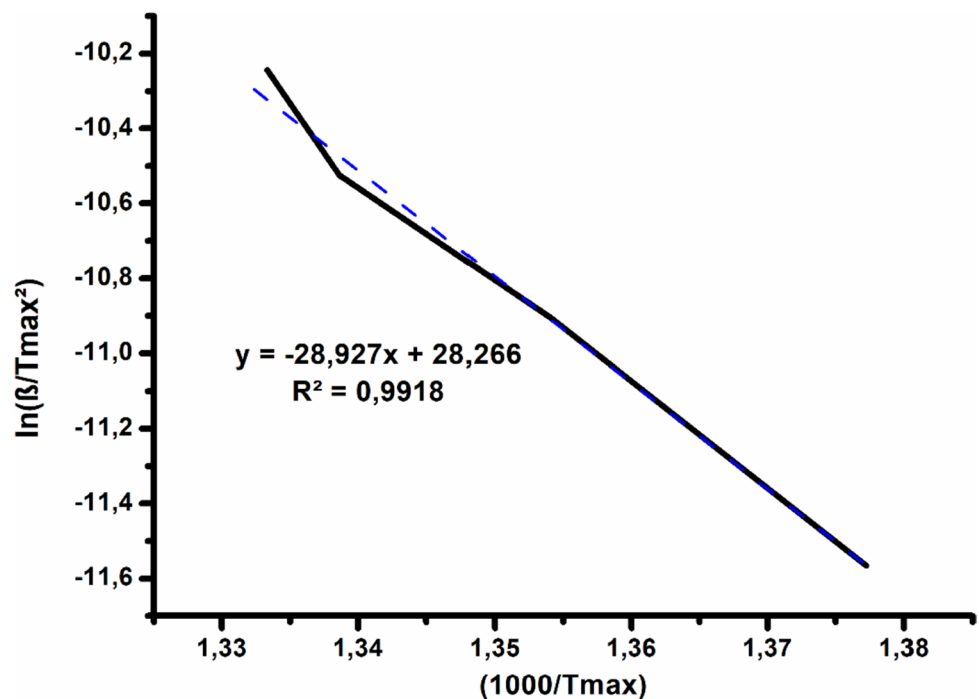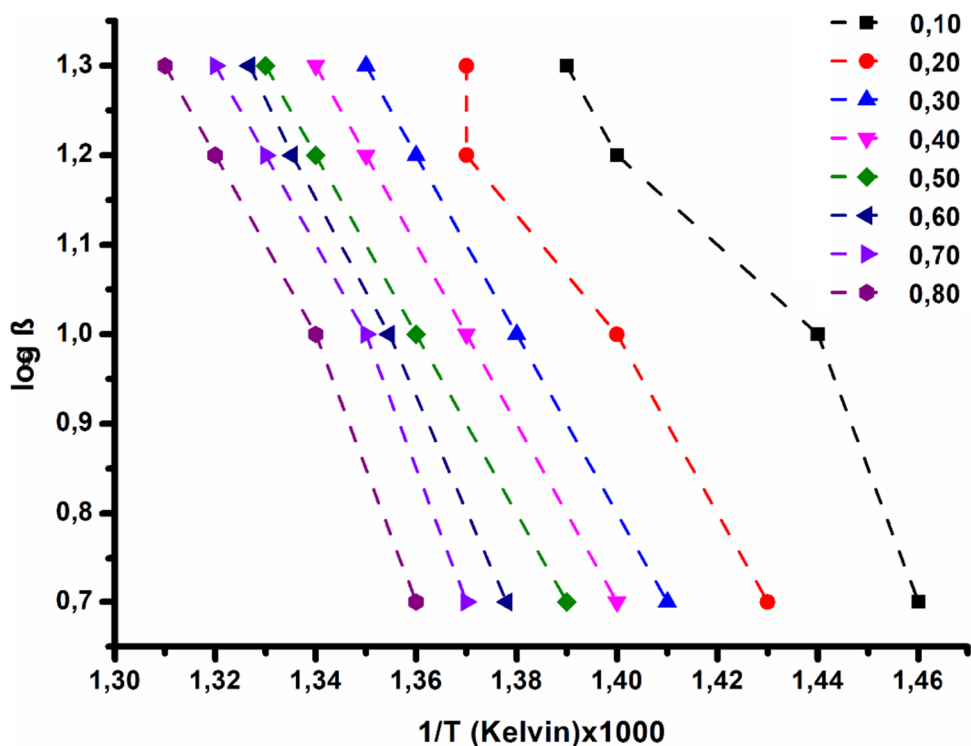$$y = -28,927x + 28,266$$
$$R^2 = 0,9918$$

Fig. 14 The logarithm of heating rate versus temperature at constant conversion (0.10, 0.20, 0.30, 0.40, 0.50, 0.60, 0.7 and 0.8) for the degradation of PP/HDPE/Zinc Borate$_{15\%}$

the first stage is due to the loss of water molecules from the surface of zinc borate molecule (approximately 4.3%). The second decay stage is between 352 and 437 °C and is about 9%. This step is due to the degradation of the crystalline water in the structure of Zinc Borate. Similar results were also found by Wu et al. When compared with the thermogram in their work using Zinc Borate ($2ZnOx3B_2O_3x3.5H_2O$), they saw a single decay with an initial temperature of 318 °C. The reason for the shift of the initial temperature of this decomposition step to 352 °C was that $2ZnOx3B_2O_3x3H_2O$, that is, the crystal structure 3 water, caused a stronger bonding and a shift in the initial temperature of the decomposition step. Zinc Borate is thermally stable after 352 °C, with 85.0% residual consisting of ZnO and B_2O_3 [7]. Although the TG of PP/HDPE/Zinc Borate$_{15\%}$ shows a single degradation step similar to PP and HDPE, its thermal stability seems to have decreased. This is thought to be because Zinc Borate weakens the interaction between PP and HDPE polymer chains and reduces the thermal stability of the mixture. The thermal stability of polymer blends depends on the composition of the respective polymers and on the ionic and covalent interactions between them. There are many factors such as functional groups, molecular weight, degree of branching, crosslinking and crystallinity in the polymer structure that affect the thermal stability of blends [46]. The decrease in the thermal stability of the PP/HDPE/Zinc Borate$_{15\%}$ composite is due to these reasons. While PP and HDPE are completely decomposed at

500 °C, the Zinc Borate molecule is present at a rate of 85% at this temperature. So, the remaining substance of our composite containing 15% zinc borate after 500 °C is the residue from Zinc Borate. The Zinc Borate ratio in our blend was calculated as 14.8% in the calculations made using the Zinc Borate molecular weight and the remaining ZnO and B_2O_3 molecular weights after the degradation of $3xH_2O$. The theoretically calculated Zinc Borate ratio in the synthesized composite has been proven by thermogravimetric analysis.

Decomposition activation energy (E_a) provides an approach used to better understand thermal decomposition behavior and thermal stability of polymer composites and blends. For this purpose, in our study, two integral methods, namely Flynn-wall-Ozawa method (FWO) and Coast Redfern, and a differential method, which is Kissenger's method, were analyzed

Table 7 Activation Energies Obtained Using the Flynn-wall-Ozawa Method

α	E_a (kJ/mol)	r^2
0.1	137	0.92
0.2	165	0.99
0.3	181	0.99
0.4	192	0.99
0.5	201	0.99
0.6	201	0.99
0.7	214	0.99
0.8	223	0.99
Mean	**189±28**	

Table 8 Activation Energies Obtained Using the Coats-Redfern Method for Several Solid-State Process

Mechanism	E (kJ/mol)	r
(a) **Heating Rate of 5 °C/min**		
A2	98	0.9984
A3	61	0.9980
A4	43	0.9975
R1	158	0.9917
R2	182	0.9983
R3	191	0.9991
D1	329	0.9922
D2	359	0.9967
D3	394	0.9992
D4	370	0.9979
F1	209	0.9987
F2	274	0.9840
F3	353	0.9588
(b) **Heating Rate of 10 °C/min**		
A2	99	0.9802
A3	62	0.9787
A4	43	0.9771
R1	161	0.9931
R2	185	0.9900
R3	193	0.9877
D1	336	0.9934
D2	365	0.9920
D3	399	0.9888
D4	376	0.9910
F1	211	0.9813
F2	275	0.9514
F3	351	0.9153
(c) **Heating Rate of 15 °C/min**		
A2	128	0.9979
A3	75	0.9974
A4	56	0.9969
R1	205	0.9885
R2	236	0.9964
R3	248	0.9977
D1	427	0.9891
D2	465	0.9943
D3	511	0.9978
D4	481	0.9959
F1	272	0.9982
F2	357	0.9862
F3	459	0.9631
(d) **Heating Rate of 20 °C/min**		
A2	126	0.9992
A3	78	0.9990
A4	55	0.9987
R1	202	0.9865
R2	232	0.9960
R3	243	0.9978

Table 8 (continued)

Mechanism	E (kJ/mol)	r
D1	419	0.9871
D2	457	0.9933
D3	502	0.9979
D4	472	0.9952
F1	267	0.9994
F2	351	0.9900
F3	452	0.9687

using. Fig. 12, TG and derivative curves (DTG) of PP/HDPE/Zinc Borate$_{15\%}$ taken in nitrogen atmosphere at 5, 10, 15, 20 °C are shown. The initial temperature (Ti) of a decomposition process, the maximum decomposition temperature (T$_{max}$), the final temperature (T$_f$) of a decomposition process and the residual mass (1-a) TG characteristics at heating rates (5 °C, 10 °C, 15 °C and 20 °C) are listed in Table 6. As shown in Fig. 12 and Table 6, the quantities of ash that remain after thermal degradation of the PP/HDPE/ZincBorate$_{15\%}$ with increasing heating rates have values between 10.6 and 11.6 for decomposition stage.

Based on differential (Kissenger method) and integral methods (Flynn-Wall-Ozawa and Coast-Redfern), kinetic parameters (activation energy and pre-exponential factor) were calculated for the PP/HDPE/Zinc Borate$_{15\%}$ in order to obtain more information about its thermal stability. In addition, kinetic studies were conducted in order to determine the mechanism of stage.

According to the method of Kissinger activation enegry was calculated from plot In (β/T$^2_{max}$) versus 1000/T$_{max}$. The activation energy and correlation obtained from the classical method of Kissinger for PP/HDPE/Zinc Borate$_{15\%}$ is 233.3 kJ/mol and r^2= 0.9912, respectively. The Kissinger plot of PP/HDPE/Zinc Borate$_{15\%}$ is given in Fig. 13. Activation energies found in the Kissinger method for virgin PP and HDPE in similar studies are 170-180 kJ·mol^{-1} and 220-230 kJ·mol^{-1}, respectively. The activation energy of the PP/HDPE/Zinc Borate$_{15\%}$ composite is about the same as that of the pure HDPE polymer, and it can be said that it has a relatively high activation energy [47–49].

Figure 14 plots logβ and 1000/T as functions of conversation using the Flynn-Wall-Ozawa method, Activation energies and correlation calculated by Flynn-Wall-Ozawa method are given in Table 7. The activation energies for the decay rates of 0.10, 0.20, 0.30, 0.40, 0.50, 0.60, 0.7 and 0.8 were calculated using the Eq. 6 and the mean value was determined as 189±28 kJ/mol. Activation energy values in studies conducted with the FWO method for pure PP and HDPE have been found to be 180-190 kJ·mol^{-1} and 230-240 kJ·mol^{-1}, respectively. The Ea value found for PP/HDPE/Zinc Borate$_{15\%}$ in this study is approximately 190 kJ·mol^{-1} and has a value equal to the average of two pure polymers [47, 49, 50].

The activation energy for all g(α) functions is represented in Table I by Coats and Redfern. Activation energies and correlation calculated by the Coats-Redfern method are given in Table 8 at different heating rate such as 5 °C, 10 °C, 15 °C and 20 °C.

As can be seen from these tables, the activation energy value calculated using the R3 mechanism (191.0 kJ/mol) is very close to Flynn-Wall-Ozawa activation energy value (189.3 kJ/mol) at 5 °C/min heating rate. The pyrolysis of HDPE was explained by the "Shrinking cylinder" model (R2) in a study [49]. The result in this study strongly suggests that the solid state thermal degradation mechanism follows the deceleration (R3) type in PP/HDPE/Zinc Borate15%.

Conclusions

In this report, new PP/HDPE/Zinc Borate composites have been synthesized using blending method and characterized using FTIR, TG-DTA, SEM-EDX and XRD. The thermal degradation of PP/HDPE-Zinc Borate$_{15\%}$ in nitrogen is one-stage reaction. Activation energies of thermal degradation of the PP/HDPE-Zinc Borate$_{15\%}$ computed with Kissinger's and Flynn–Wall– Ozawa method in a nitrogen atmosphere were 233.3 and 189.3kJ/mol. respectively. Analysis of the experimental conclusions proposed that the reaction mechanism was R_3 deceleration type that is phase boundary controlled reaction (contraction volume). When the compare PP, HDPE and PP/HDPE-Zinc Borate's thermal resistance, PP/HDPE-Zinc Borate's is higher than that of pure PP or HDPE. Some important information necessary to characterize and control product performance is provided by rheological analysis. According to the results obtained from here, PP/HDPE/Zinc Borate$_{15\%}$ composite can maintain its plasticity under a certain force. The molecular structure does not undergo much degradation.

Data availability The authors declare that the data supporting the findings of this study are available within the paper and its Supplementary Information files. Should any raw data files be needed in another format they are available from the corresponding author upon reasonable request.

Declarations

Conflict of interest The authors declare that they have no known competing financial interests or personal relationships that could have appeared to influence the work reported in this paper.

References

1. Xiao D, Gohs U, Wagenknecht U, Voit B, Wang D-Y (2022) Thermal stability and pyrolysis behavior of an efficient fire-retarded polypropylene containing allylamine polyphosphate and pentaerythritol. Thermochim Acta 708

2. Jiang Y, Zhai C, Shi L, Liu X, Gong J (2021) Assessment of melting and dripping effect on ignition of vertically discrete polypropylene and polyethylene slabs. J Therm Anal Calorim 144:751–762

3. Sirin M, Zeybek MS, Sirin K, Abali Y (2022) Effect of gamma irradiation on the thermal and mechanical behaviour of polypropylene and polyethylene blends. Radiat Phys Chem 194

4. Brant P, Brown GM, Narvaez A (2022) Impact of order of catalytic ethylene and propylene polymerization on nanometer scale isotactic polypropylene-polyethylene blend morphology in nascent heterophasic granules revealed by low voltage scanning electron microscopy and scanning transmission electron microscopy. J Appl Polym Sci 139:51938

5. Jing X, Li Y, Zhu J, Chang L, Maganti S, Naik N, Xu BB, Murugadoss V, Huang M, Guo Z (2022) Improving thermal conductivity of polyethylene/polypropylene by styrene-ethylene-propylene-styrene wrapping hexagonal boron nitride at the phase interface. Adv Compos Hybrid Mater 5:1090–1099

6. Liu X-X, Huang Y-Z, Huang Z-X (2022) Compatibilizing and functionalizing polypropylene/polyethylene by *in-situ* exfoliating hexagonal boron nitride at interface. Compos Sci Technol 221

7. Wu Q, Guo J, Fei B, Li X, Sun J, Gu X, Li H, Zhang S (2020) Synthesis of a novel polyhydroxy triazine-based charring agent and its effects on improving the flame retardancy of polypropylene with ammonium polyphosphate and zinc borate. Polym Degrad Stabil 175

8. Mu JJ, Zhou R, Liu C, Su T (2021) Synergistic effect of intumescent flame retardant and zinc borate on linear low-density polyethylene. Polym Eng Sci 61:2820–2830

9. Xu Y, Zhou R, Mu J, Ding Y, Jiang J (2022) Synergistic flame retardancy of linear low-density polyethylene with surface modified intumescent flame retardant and zinc borate. Colloid Surf A 640

10. Chen X, Yu J, Luo Z, Hu S, Zhou Z, Guo S, Lu S (2009) Kinetics of thermo-oxidative degradation of zinc borate/microcapsulated red phosphorus with magnesium hydroxide in flame retarded polypropylene composites. J Polym Res 16:745–753

11. Wu Z, Hu Y, Shu W (2009) Influence of Ultrafine Zinc Borate on the thermal degradation behavior of a(low-Density polyethylene)/(Intumescent Flame Retardant) System. J Vinyl Addit Techn 15:260–265

12. Gonnella G, Ischia G, Fambri L, Fior L (2022) Thermal analysis and kinetic modeling of Pyrolysis and Oxidation of Hydrochars. Energies 15

13. Ganiyu SO, Sable S, El-Din MG (2022) Advanced oxidation processes for the degradation of dissolved organics in produced water: a review of process performance, degradation kinetics and pathway. Chem Eng J 429

14. Rathore NS, Pawar A, Panwar NL (2021) Kinetic analysis and thermal degradation study on wheat straw and its biochar from vacuum pyrolysis under non-isothermal condition. Biomass Conv Bioref https://doi.org/10.1007/s13399-021-01360-w

15. Thomas A, Moinuddin K, Tretsiakova-McNally S, Joseph PA (2020) Kinetic analysis of the thermal degradation behaviours of some bio-based substrates. Polymers 12

16. Kissinger HE (1956) Variation of peak temperature with heating rate in differential thermal analysis. J Res Natl Bur Stand 57:217–221

17. Kissinger HE (1957) Reaction kinetics in differential thermal analysis. Anal Chem 29:1702–1706

18. Vyazovkin S (2020) Kissinger method in kinetics of materials: things to beware and be aware of. Molecules 25

19. Popescu C (1996) Integral method to analyze the kinetics of heterogeneous reactions under non-isothermal conditions a variant on the Ozawa-Flynn-Wall method. Thermochim Acta 285:309–323

20. Dowdy DR (1987) Meaningful activation energies for complex systems-I. The application of the Ozawa-Flynn-Wall method to multiple reactions. J Therm Anal 32:137–147

21. Naqvi SR, Tariq R, Hameed Z, Ali I, Naqvi M, Chen W-H, Ceylan S, Rashid H, Ahmad J, Taqvi SA, Shahbaz M (2019) Pyrolysis of high ash sewage sludge: kinetics and thermodynamic analysis using Coats-Redfern method. Renew Energ 131:854–860

22. Ou CY, Zhang CH, Li SD, Yang L, Dong JJ, Mo XL, Zeng MT (2010) Thermal degradation kinetics of chitosan–cobalt complex as studied by thermogravimetric analysis. Carbohyd Polym 82:1284–1289

23. Hatakeyama T, Quinn FX (1999) Thermal analysis: fundamentals and applications to polymer science. John Wiley & Sons Ltd, Chichester

24. Criado JM, Malek J, Ortega A (1989) Applicability of the master plots in kinetic analysis of non-isothermal data. Thermochim Acta 147:377–385

25. Montserrat S, Málek J, Colomer P (1998) Thermal degradation kinetics of epoxy–anhydride resins: I.: influence of a silica filler. Thermochim Acta 313:83–95

26. Prabowo I, Pratama JN, Chalid M (2017) The effect of modified ijuk fibers to crystallinity of polypropylene composite. IOP Conf Ser: Mater Sci Eng 223:012020

27. Gulmine JV, Janissek PR, Heise HM, Akcelrud L (2002) Polyethylene characterization by FTIR. Polym Test 21:557–563

28. Tan VT, Vinh LT, Quynh LT, Suong HT, Chinh HD (2020) A novel synthesis of nanoflower-like zinc borate from zinc oxide at room temperature. Mater Res Express 7:015059

29. Madhu G, Bhunia H, Bajpai PK, Chaudhary V (2014) Mechanical and morphological properties of high density polyethylene and polylactide blends. J Polym Eng 34:813–821

30. Liao YJ, Wu XLi, Peng X, Zhou Z, Wu JZ, Wu F, Jiang T, Chen JX, Zhu L, Yi T (2019) Enhancing the mechanical and thermal properties of polypropylene composite by encapsulating styrene acrylonitrile with ammonium polyphosphate. BMC Chem 13:9

31. Aumnate C, Rudolph N, Sarmadi M (2019) Recycling of Polypropylene/Polyethylene blends: Effect of Chain structure on the crystallization behaviors. Polymers 11

32. Köytepe S, Vural S, Seçkin T (2009) Molecular design of nanometric zinc borate-containing polyimide as a route to flame retardant materials. Mater Res Bull 44:369–376

33. Kaczmarek H, Chylińska M, Królikowski B, Klimiec E, Bajer D, Kowalonek J (2019) Infuence of glass beads fller and orientation process on piezoelectric properties of polyethylene composites. J Mater Sci-Mater El 30:21032–21047

34. Zhang L, Zhang J, Yue Z, Li L (2016) New three-phase polymer-ceramic composite materials for miniaturized microwave antennas. AIP Adv 6:095319

35. Wang S, Ajji A, Guo S, Xiong C (2017) Preparation of Microporous Polypropylene/Titanium Dioxide Composite membranes with enhanced Electrolyte Uptake Capability via Melt Extruding and stretching. Polymers 9

36. Lin J-H, Pan Y-J, Liu C-F, Huang C-L, Hsieh C-T, Chen C-K, Lin Z-I, Lou C-W (2015) Preparation and compatibility evaluation of Polypropylene/High density polyethylene polyblends. Materials 8:8850–8859

37. Liang P, Tuoheti Z, Liu Z-H (2017) Controlling the structure and morphology of zinc borate by adjusting the reaction temperature and pH value: formation mechanisms and luminescent properties. RSC Adv 7:3695–3603

38. Chen W, Li H, Li L, Wang X (2020) Reinforcing condensed phase flame retardancy through Surface Migration of Brucite@Zinc Borate-Incorporated Systems. ACS Omega 5:28186–28195

39. Saltan F (2021) Preparation of poly(eugenol-co-methyl methacrylate)/polypropylene blend by creative route approach: structural and thermal characterization. Iran Polym J 30:1227–1236

40. Sultan Md T, Haque Md M-U, Maniruzzaman M, Alam Md A (2015) Composites of polypropylene with pulque fibres: morphology, thermal and mechanical properties. J Thermoplast Compos 28:1615–1626

41. Frida E, Bukit N, Zebua F (2014) Analysis mechanics and thermal Composites Thermoplastic High Density Polyethylene with Zeolite Modification Filler. Chem Mater Res 6:126–134

42. Li S, Long B, Wang Z, Tian Y, Zheng Y, Zhang Q (2010) Synthesis of hydrophobic zinc borate nanoflakes and its effect on flame retardant properties of polyethylene. J Solid State Chem 183:957–962

43. Bingham EC (1922) Fluidity and plasticity. MC Graw-hill, New York

44. Schramm LL (2006) Emulsions, foams and suspensions: Fundamentals and Applications. John Wiley & Sons Inc, Weinheim

45. Awad AH, El-Wahab AAA, El-Gamsy R, Abdel-latif MH (2019) A study of some thermal and mechanical properties of HDPE blend with marble and granite dust. Ain Shams Eng J 10:353–358

46. Tomić NZ (2020) Thermal studies of compatibilized polymer blends. Compatibilization of polymer blends 489 – 10

47. Briceno J, Lemos MA, Lemos F (2021) Kinetic analysis of the degradation of HDPE + PP polymer mixtures. Int J Chem Kinet 53:660–674

48. Aboulkas A, El Harfi K, El Bouadili A (2010) Thermal degradation behaviors of polyethylene and polypropylene. Part I: pyrolysis kinetics and mechanisms. Energy Convers Manag 51:1363–1369

49. Aboulkas A, El Harfi K, El Bouadili A, Benchanaa M, Mokhlisse A, Outzourit A (2007) Kinetics of Co-Pyrolysis of Tarfaya (Morocco) Oil Shale with High-Density Polyethylene. Oil Shale 24:15–33

50. Wu CH, Chang CY, Hor JL, Shih SM, Chen LW, Chang FW (1993) On the thermal treatment of plastic mixtures of MSW: pyrolysis kinetics. Waste Manag 13:221–235